Neurobiology of Disease

Persistent Adaptations in Afferents to Ventral Tegmental Dopamine Neurons after Opiate Withdrawal

Jennifer Kaufling and Gary Aston-Jones
Medical University of South Carolina, Charleston, South Carolina 29425

Protracted opiate withdrawal is accompanied by altered responsiveness of midbrain dopaminergic (DA) neurons, including a loss of DA cell response to morphine, and by behavioral alterations, including affective disorders. GABAergic neurons in the tail of the ventral tegmental area (tVTA), also called the rostromedial tegmental nucleus, are important for behavioral responses to opiates. We investigated the tVTA–VTA circuit in rats after chronic morphine exposure to determine whether tVTA neurons participate in the loss of opiate-induced disinhibition of VTA DA neurons observed during protracted withdrawal. *In vivo* recording revealed that VTA DA neurons, but not tVTA GABAergic neurons, are tolerant to morphine after 2 weeks of withdrawal. Optogenetic stimulation of tVTA neurons inhibited VTA DA neurons similarly in opiate-naive and long-term withdrawn rats. However, tVTA inactivation increased VTA DA activity in opiate-naive rats, but not in withdrawn rats, resembling the opiate tolerance effect in DA cells. Thus, although inhibitory control of DA neurons by tVTA is maintained during protracted withdrawal, the capacity for disinhibitory control is impaired. In addition, morphine withdrawal reduced both tVTA neural activity and tonic glutamatergic input to VTA DA neurons. We propose that these changes in glutamate and GABA inputs underlie the apparent tolerance of VTA DA neurons to opiates after chronic exposure. These alterations in the tVTA–VTA DA circuit could be an important factor in opiate tolerance and addiction. Moreover, the capacity of the tVTA to inhibit, but not disinhibit, DA cells after chronic opiate exposure may contribute to long-term negative affective states during withdrawal.

Key words: addiction; dopamine; morphine; RMTg; tVTA; ventral tegmental area

Significance Statement

Dopaminergic (DA) cells of the ventral tegmental area (VTA) are the origin of a brain reward system and are critically involved in drug abuse. Morphine has long been known to affect VTA DA cells via GABAergic interneurons. Recently, GABAergic neurons caudal to the VTA were discovered and named the tail of VTA (tVTA). Here, we show that tVTA GABA neurons lose their capacity to disinhibit, but not to inhibit, VTA DA cells after chronic opiate exposure. The failure of disinhibition was associated with a loss of glutamatergic input to DA neurons after chronic morphine. These findings reveal mechanisms by which the tVTA may play a key role in long-term negative affective states during opiate withdrawal.

Introduction

Dopaminergic (DA) neurons of the ventral tegmental area (VTA) play a crucial role in motivated behaviors (Wise, 2004; Fields et al., 2007) and drug addiction (Lüscher and Malenka, 2011; Volkow et al., 2011). Several results link opiate reward with VTA DA neurons: opiates activate these cells (Wise, 1989; Georges et al., 2006), and μ opioid receptor agonists are self-administered directly into the VTA (Devine and Wise, 1994; Zangen et al., 2002) in which they also produce a conditioned place preference (Phillips and LePiane, 1980; Bals-Kubik et al., 1993).

Opiates activate VTA DA neurons by inhibiting local GABA interneurons (Gysling and Wang, 1983; Johnson and North, 1992a,b). Recent results indicate that opiates can also activate VTA DA neurons by inhibiting GABA inputs from outside the VTA (Jalabert et al., 2011; Matsui and Williams, 2011; Margolis et al., 2012; Hjelmstad et al., 2013). Here, we investigated the role of GABA neurons in the tail of the VTA (tVTA), in morphine effects on VTA DA neural activity.

The tVTA (also known as the rostromedial tegmental nucleus) is a GABAergic area caudal to the VTA (Kaufling et al., 2009, Jhou et al., 2009b) that provides strong inhibitory control

Received Feb. 20, 2015; revised May 22, 2015; accepted May 29, 2015.

Author contributions: J.K. and G.A.-J. designed research; J.K. performed research; J.K. analyzed data; J.K. and G.A.-J. wrote the paper.

This research was supported by National Institutes of Health Grant R37/R01 DA006214. We thank Drs. Stephen V. Mahler and Elena Vazey for their comments on the manuscript.

Correspondence should be addressed to Gary Aston-Jones at his present address: Brain Health Institute, Rutgers University/Rutgers Biomedical and Health Sciences, Room 259 SPH, 683 Hoes Avenue West, Piscataway, NJ 08854. E-mail: aston.jones@rutgers.edu.

J. Kaufling's present address: Medical Research Council Brain Network Dynamics Unit, University of Oxford, Mansfield Road, Oxford OX1 3TH, UK.

DOI:10.1523/JNEUROSCI.0715-15.2015

 0270-6474/15/3510290-14$15.00/0

of the mesolimbic DA system (for review, see Lavezzi and Zahm, 2011; Bourdy and Barrot, 2012). Both *in vivo* electrical stimulation (Jalabert et al., 2011; Lecca et al., 2012) and *in vitro* optogenetic stimulation of the tVTA (Matsui and Williams, 2011) inhibit VTA DA neuron firing, which confirm the inhibitory control of VTA DA neurons by the tVTA.

The tVTA has been proposed to mediate the acute effects of morphine on VTA DA neurons. Rats self-administered μ receptor agonists directly into the tVTA, showing that the tVTA can drive reward (Jhou et al., 2012), and inhibition of VTA DA neurons induced by electrical or optogenetic stimulation of the tVTA is reduced by morphine (Jalabert et al., 2011; Matsui and Williams, 2011; Lecca et al., 2012). Furthermore, pharmacological tVTA inhibition blocks VTA DA activation induced by intravenous morphine (Jalabert et al., 2011).

Thus, studies reveal that tVTA is a site of action for acute morphine, but none investigated the effect of chronic morphine and morphine withdrawal on tVTA GABA neurons or the role of the effects of morphine in the tVTA on DA VTA neurons *in vivo*. This is important because the VTA is also implicated in motivational and affective components of opiate withdrawal (Harris and Aston-Jones, 2003b; Aston-Jones et al., 2010; Richardson and Aston-Jones, 2012 Lutz and Kieffer, 2013). Here we compared the effects of acute, chronic opiates, or opiate withdrawal, on activity of VTA DA and tVTA GABA neurons and on the response of VTA DA neurons to tVTA activation. We confirm that VTA DA neurons express tolerance to morphine after chronic administration (Georges et al., 2006). Surprisingly, this was not the case for tVTA neurons, indicating that the regulation of VTA DA neurons by tVTA was altered by morphine withdrawal. Our data indicate that this dysregulation is attributable to reduced activity of tVTA neurons and reduced glutamatergic tone in the VTA in withdrawn rats.

Materials and Methods

Animals. Male Sprague Dawley rats were used (300–450 g; Charles River Laboratories; $n = 153$ for electrophysiological procedures, $n = 12$ for anatomical procedures, $n = 14$ for optogenetic procedures). Rats were singly housed (22–23°C; 12 h light/dark cycle, lights on 7:00 A.M.) with food and water available *ad libitum*. All protocols and procedures followed National Institute of Health *Guidelines for the Care and Use of Laboratory Animals* and were approved by the Medical University of South Carolina Institutional Animal Care and Use Committee.

Chronic morphine treatment. Two 75 mg morphine pellets (provided by the National Institute on Drug Abuse, National Institutes of Health) were implanted subcutaneously under isoflurane anesthesia for chronic morphine treatment. This procedure has been shown to produce a consistent plasma morphine concentration beginning a few hours after the implantation of the pellets (Yoburn et al., 1985) and physical dependence, including overt somatic withdrawal signs after an acute injection of opiate antagonist (Frenois et al., 2002). Full behavioral dependence on morphine is achieved 24 h after implantation of the morphine pellets and remains relatively constant for 15 d (Gold et al., 1994). On the basis of these physiological and behavioral findings, we used the term "morphine dependent" (MD) to denote rats implanted chronically with two pellets of morphine for at least 6 d. Pellets remained in this group during recording experiments. The drug-naive rats (naive) received placebo pellets without morphine ($n = 20$) or were not implanted ($n = 51$); there was no difference in results between animals with placebo pellets or no pellets, and, therefore, results were pooled. Electrophysiological experiments in MD rats were performed 6 d after the implantation of morphine pellets ($n = 32$). Precipitated withdrawal was induced by intravenous injection of naltrexone hydrochloride (NAL; 0.1 mg/kg in saline; Sigma), and unit recordings were obtained during 3 h after NAL administration ($n = 23$). Protracted withdrawal (14DW group) was induced by removing morphine pellets after 6 d, and electrophysiological experiments were performed 14 d later ($n = 16$).

Intravenous drug injection. During terminal intracranial surgery, the jugular vein was cannulated for intravenous administration of pharmacological agents. NAL (0.1 mg/kg per 0.5 ml) and morphine hydrochloride (1 mg/kg per 0.5 ml) were prepared in isotonic saline.

Surgery. Animals were anesthetized initially with 3% isoflurane, a tracheotomy was performed, and 1.5% isoflurane was delivered through a tracheal cannula via spontaneous respiration for surgical procedures. During recording experiments, the concentration of isoflurane was kept at 1.0–1.2%. Animals were placed in a stereotaxic frame, and body temperature was maintained at 36–38°C with a thermistor-controlled electric heating pad. The skull was exposed, and holes were drilled above the tVTA (window: 6.7/7.5 mm caudal to bregma, 0.3/0.7 lateral to bregma, and 6.0/8.0 ventral to dura) or the VTA (window: 5.2/6.0 mm caudal to bregma, 0.4/1.0 lateral to bregma, and 7.5/−9.5 ventral to the dura). To allow VTA recording during tVTA pharmacological manipulation, some tVTA injection pipettes were angled 6° from vertical (rostrodorsal to caudoventral).

Electrophysiological methods. A glass micropipette (1–3 μm, 6–12 MΩ) filled with 2.0% pontamine sky blue (BDH Chemicals) in 0.5 M sodium acetate was used for VTA and tVTA recording. Signals were amplified and filtered (0.1–5 kHz bandpass) with conventional electronics. Spikes of single neurons were discriminated, and digital pulses were sent to a computer for online data collection with a laboratory interface and software (CED 1401, Spike2; Cambridge Electronic Design). Only spontaneously active neurons were recorded and analyzed. Neurons were recorded for 2 min to establish a mean baseline firing rate before any pharmacological manipulation.

Double-barrel micropipettes were custom fabricated as described previously (Akaoka and Aston-Jones, 1991; Georges and Aston-Jones, 2002) to allow simultaneous VTA or tVTA neuron recordings with local microinjection of drugs. The recording micropipette (tip diameter, 1–3 μm; 6–12 MΩ) was filled with 2.0% pontamine sky blue in 0.5 M sodium acetate. The injection pipette (30–40 μm tip diameter, offset 150 μm behind the recording pipette tip) was filled with drugs or vehicles (see below, Intracranial drug administration). After at least 2 min of stable recording, drug or vehicle was microinfused via pneumatic pressure (Picospritzer; General Valve) at a rate of 30–60 nl/min for 1–2 min, and effects on spontaneous impulse activity were recorded. For local tVTA injection without recording, a single injection pipette was used.

For VTA recordings, electrophysiological criteria used to identify putative DA neurons were similar to previous studies (Grace and Bunney, 1984a,b; Ungless et al., 2004; Ungless and Grace, 2012). These included the following: (1) action potential with biphasic or triphasic waveform $\geq$2.5 ms in duration; (2) $\geq$1.1 ms from spike onset to negative trough; and (3) slow spontaneous firing rate $<$10 spikes/s. It was critical to locate precisely the tVTA and define its borders to confirm our recordings, photostimulation, and chemical inhibition in that structure. We used GAD and μ opioid receptor immunochemistry to map and verify the localization of each tVTA recorded cell. As in previous reports (Jalabert et al., 2011; Lecca at al., 2011, 2012), we considered tVTA units to be putative GABA neurons if the early spike duration (peak to initial negative trough) was $\leq$1.1ms (mean $\pm$ SEM, 0.65 $\pm$ 0.017 ms in our study). tVTA GABA cells are reported to have highly variable basal firing rates (ranging from 1 to 60 Hz in the study by Jalabert et al., 2011), and, therefore, we did not use this parameter to identify them. In addition, we evaluated the proportion of GABA neurons throughout the tVTA area using GAD immunochemistry. With our histological localization of recording sites, this analysis allowed us to define GABA neuron recordings as originating from an area in the tVTA in which $>$75% of neurons are GAD positive (GAD^+; Fig. 1). We also removed from our tVTA analysis any recordings with parameters of classical DA neurons, accounting for $\sim$12% of tVTA recorded cells. Although we recognize that it is not possible to absolutely identify GABA neurons without intracellular or juxtacellular labeling, together these multiple criteria allowed us to conclude that $>$87% of the tVTA neurons we tentatively identified as GABAergic were in fact GABA cells.

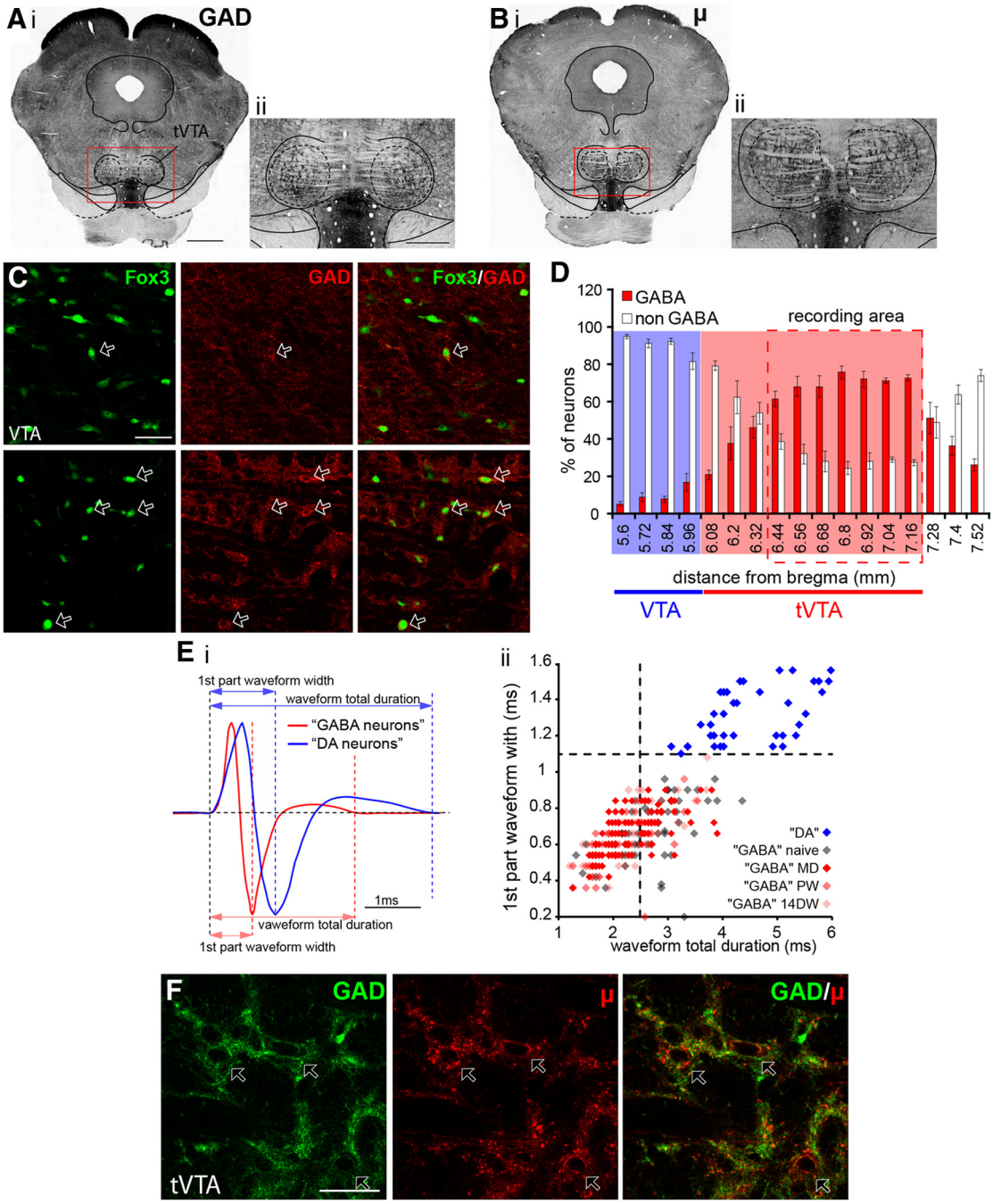

Figure 1. Localization of recorded GABA neurons in the tVTA. ***A***, ***B***, Light microscopy photographs showing staining for GAD (***Ai***, low-power view; ***Aii***, high-power of area in red box in ***Ai***) and μ receptors (***Bi***, low-power view; ***Bii***, high-power of area in red box in ***Bi***) in coronal slices through the tVTA. Staining for GAD or μ receptors highlights the tVTA (outlined with black dashed lines in ***A*** and ***B***). ***C***, Fluorescence microscopy photographs of staining for neurons (revealed by Fox3, green), GAD (red), and merged images in the VTA (top row) and tVTA (bottom row). Arrows indicate examples of GABA (GAD$^+$) neurons. Note that the tVTA contains more GABA neurons than the VTA. ***D***, Bar graph illustrating the proportion of GABA neurons throughout the rostrocaudal extent of the VTA–tVTA (plotted as proportion of Fox3$^+$ neurons that are also GAD$^+$; $n = 3$ rats, 6 hemispheres). The *x*-axis shows approximate anteroposterior distance from bregma (in millimeters). The red shaded area denotes tVTA as defined by Kaufling et al. (2009). The red dashed line defines the tVTA recording area used here, in which >75% of the neurons are GABAergic (GAD$^+$). ***Ei***, Typical example of average spike waveform of putative DA and GABA neurons recorded in the tVTA. Putative GABA-like spike waveforms are shorter than for putative DA neurons. ***Eii***, Scatter plot illustrates the width of the first part of the action potential (AP) as a function of AP total duration for all tVTA recorded neurons. Two populations are clearly distinguishable. Classical AP waveforms for DA neurons are shown in blue (first part AP duration $\geq$1.1 ms and AP total duration $\geq$2.5 ms). Typical GABA-like waveforms are plotted in red and gray (corresponding to cells recorded in naive, PW, or 14DW rats). Note that chronic morphine treatment did not affect the AP duration of tVTA GABA neurons recorded ($F_{(3,269)} = 2.02$, ns). ***F***, High-power fluorescence photographs of immunohistochemistry for GAD (green) and μ receptors (red) in the tVTA. The merged image (GAD/μ) shows that GABA neurons express μ receptors (examples at arrows). Scale bars: ***Ai***, ***Bi***, 1 mm; ***Aii***, ***Bii***, 500 μm; ***C***, 15 μm; ***F***, 100 μm.

Intracranial drug administration. Double-barrel micropipettes consisted of a recording micropipette (described above) glued to an injection micropipette. The injection micropipettes had tip diameters of 30–40 μm and were filled with either 100 μM DAMGO in ACSF or with a mixture of 100 μM AP-5 and 50 μM CNQX in ACSF. The concentrations of DAMGO and CNQX/AP-5 were based on previous studies of DA neurons *in vivo* or *in vitro* (Georges and Aston-Jones, 2002; Matsui and Williams, 2011). Drugs or vehicle were ejected by brief pulses of pneu-

matic pressure (60 nl at 30–60 nl/min). At least 45 min separated any two drug infusions. For tVTA inactivation during VTA recording, single-barrel injection micropipettes were used to microinfuse muscimol bodipy (MusB; a fluorescent $GABA_A$ agonist; 500 nl, 0.8 mM in ACSF) into the tVTA. VTA neurons were recorded during 2 h after MusB injection, as in previous studies (Jalabert et al., 2011).

Optogenetic methods. Channelrhodopsin2 (ChR2) was expressed in neurons using adeno-associated virus (AAV) constructs. The vector AAV2/5–CaMKIIa–hChR2(H134R)–eYFP (60 nl; 1.28 e^{13} viral particles/μl; University of North Carolina Vector Core Facility) was injected unilaterally by micropressure (Picospritzer) using a glass micropipette (40 μm tip diameter) into the tVTA (from bregma, −6.8 mm posterior, 1.1 mm mediolateral, −7.8 mm ventral, 6° lateral angle). This virus injection procedure resulted in injection sites that were restricted to the tVTA, resulting in ChR2 prominently in GABA neurons there and in fibers/terminals in the VTA (see Fig. 6*B*). One week after virus injection, animals were divided in two groups: naive and 14DW (see above, Chronic morphine treatment). In all experiments, recordings were conducted >4 weeks after virus injections.

To determine the effect of tVTA optogenetic stimulation on VTA DA activity, a 200 μm optical fiber was inserted stereotaxically 400 μm above the tVTA virus injection site while VTA neurons were recorded. To confirm the effect of tVTA optogenetic stimulation directly on tVTA neurons, a 200 μm optical fiber was glued onto the tVTA recording pipette, ending 350 μm above the tip. After baseline recording of the spontaneous activity of the VTA or tVTA cells for at least 2 min, a 473 nm blue laser (300 mW; OEM Laser Systems) was used to photostimulate tissue (10 ms light pulse, 1 Hz, 100 repetitions). Light intensity at the optical fiber tip was ~10 mW.

Histology and immunohistochemistry. At the end of each recording experiment, electrode

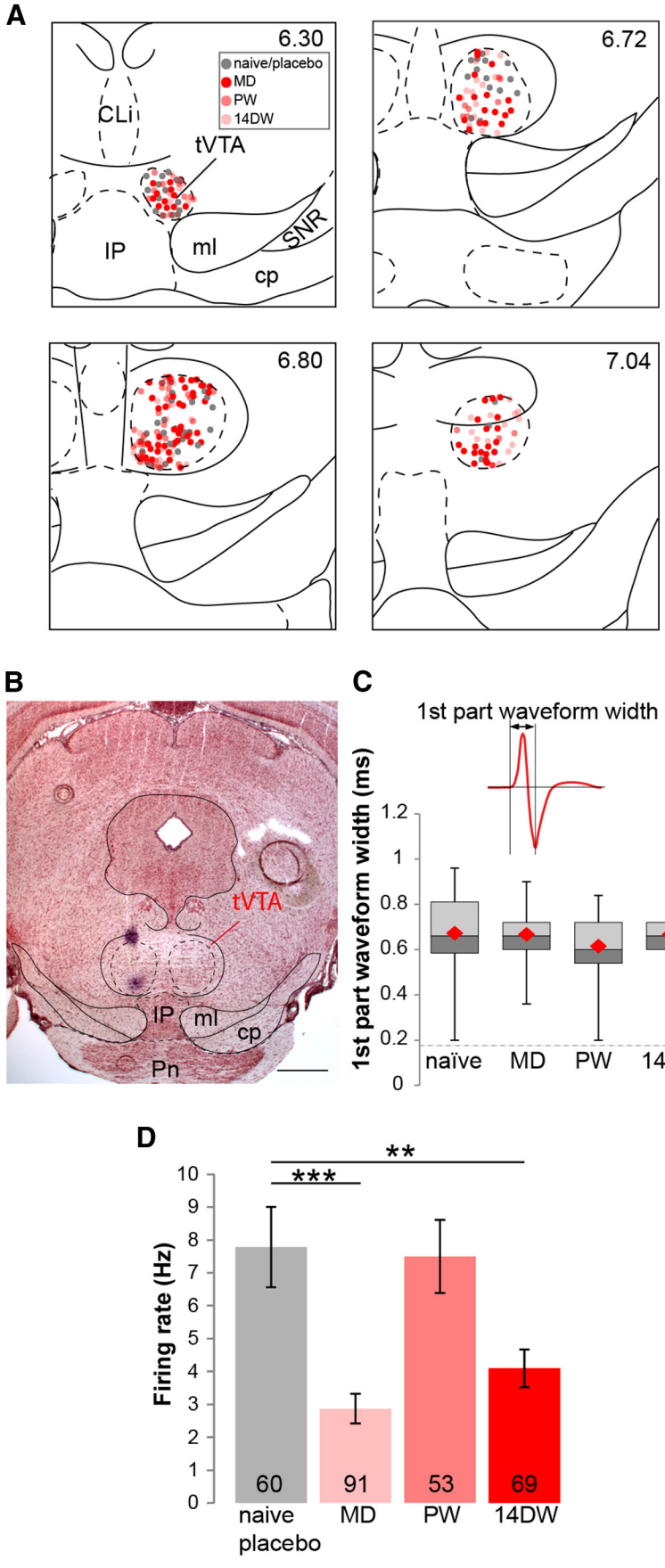

Figure 2. The firing rate of tVTA GABA neurons is lower in MD and PW animals than in naive rats. ***A***, Schematics showing the localization of each tVTA GABA-like neuron recorded. Landmarks and position from bregma in millimeters (adapted from Paxinos and Watson, 2007). ***B***, Photograph of a frontal section (neutral red stain) showing pontamine sky blue deposits made at the top and the bottom of a tVTA recording electrode track. Scale bar, 1 mm. ***C***, Inset, Typical example of tVTA GABA-like neuron waveform. The width of the first waveform component was measured from the start of the spike to the negative trough, which was 0.65 ms in this example. Whisker plots show that the width of the first waveform component for putative GABAergic neurons were similar in all treatment groups. ***D***, Bar graph showing the basal firing rates of tVTA GABA-like neurons in different treatment groups. Basal firing rates in MD and 14DW rats were lower than in naive/placebo rats. Intravenous NAL (0.1 mg/kg) in dependent rats (PW rats) normalized the basal firing rate. For all figures: naive/placebo rats, $n = 60$ cells, 20 rats; MD rats, $n = 91$ cells, 32 rats; PW rats, $n = 53$ cells, 23 rats; 14DW rats, $n = 70$ cells, 16 rats). $^{**}p < 0.01$; $^{***}p < 0.001$. CLi, caudal linear nucleus of the raphe; cp, cerebral peduncle; IP, interpeduncular nucleus; ml, medial lemniscus; Pn, pontine nuclei; SNR, substantia nigra pars reticulata.

placement was marked with an iontophoretic deposit of pontamine sky blue dye (−7 μA, pulsed current for 15 min). After the experimental procedures, the animals were anesthetized deeply with isoflurane (5%) and decapitated. Brains were removed and snap-frozen in a solution of methyl butane at −70°C. Coronal, 40-μm-thick sections were cut on a cryostat and counterstained with neutral red (Thermo Fisher Scientific), dehydrated with graded alcohol solutions, cleared with xylene, and coverslipped with Permount (Thermo Fisher Scientific). In the case of tVTA recording, two blue spots (top and bottom of the last track) were made to precisely localize recorded neurons. Only tVTA or VTA neurons from rats with histologically confirmed recording sites were analyzed.

To localize MusB injections in the tVTA, animals were perfused with cold 0.09% NaCl, followed by cold 4% paraformaldehyde in 0.1 M phosphate buffer (PB). Brains were postfixed overnight in 4% paraformaldehyde and transferred to a 20% solution of sucrose/0.1% sodium azide in PB at 4°C for at least 3 d. Coronal 40-μm-thick sections of brains were cut on a cryostat. VTA/tVTA sections were mounted onto slides and coverslipped with anti-fade mounting solution. Sections were examined with a Leica DM-RXA microscope (Leica Microsystems). Photomicrographs were acquired with a CCD camera (Princeton Instruments) and processed using OpenLab imaging software (Improvision; PerkinElmer Life and Analytical Sciences). Adobe Photoshop CS version 8.0 was used to adjust contrast, brightness, and sharpness. The color channels were adjusted individually for the merged pictures. Abbreviations and structure limits are based on the frontal diagrams from the atlas of Paxinos and Watson (2007).

To localize the rostrocaudal extent of the tVTA and to show that tVTA GABA cells express μ opioid receptors, four series of sections through the VTA and tVTA were processed by immunochemistry, as described in detail below. GAD67 and μ receptors were visualized by 3,3-diaminobenzidine (DAB; $n = 3$), and GAD/μ receptor and GAD/Fox3 double immunochemistry were revealed by immunofluorescence ($n = 3$). This last series allowed us to evaluate the proportion of tVTA neurons (revealed by Fox3) that are GABAergic. To confirm the localization of tVTA virus expression, dual immunofluorescence for enhanced yellow fluorescent protein (eYFP; to reveal ChR2-expressing neurons) with either GAD (to reveal tVTA borders) or tyrosine hydroxylase (TH; to localize VTA) were done. Animals were perfused as described above. Coronal 40-μm-thick sections of the VTA/tVTA were cut on a cryostat; one in four sections was used for each staining series.

For immunohistochemical processing, sections were washed in PBS (three times for 10 min), incubated 15 min in a 1% H_2O_2/50% ethanol solution if used for a DAB reaction, washed in PBS (three times for 10 min), and incubated in PBS containing Triton X-100 and 5% donkey serum for 45 min. Sections were then incubated overnight at room temperature in PBS with 0.5% Triton X-100, 1% donkey serum, and primary antibodies. Five primary antibodies were used, as follows: (1) mouse anti-GAD 67 kDa monoclonal antibody (1:10,000 for DAB and for immunofluorescent staining; catalog #MAB5406; Millipore Bioscience Research Reagents), which is raised against a recombinant fusion protein containing N-terminal regions of GAD67 kDa not shared by GAD65 kDa (Millipore Bioscience Research Reagents data sheet); (2) guinea pig anti-μ receptor polyclonal antibody (1:5000 for DAB reaction, 1:2500 for immunofluorescent staining; catalog #AB5509; Millipore Bioscience Research Reagents); (3) rabbit anti-Fox3 polyclonal antibody (1:1000 for immunofluorescent staining; catalog #ab104225; Abcam); (4) chicken anti-eYFP polyclonal antibody (1:2000; catalog #ab13970; Abcam); and (5) rabbit anti-TH polyclonal antibody (1:1000; catalog #AB152; Millipore Bioscience Research Reagents).

Sections for immunofluorescence were washed in PBS (three times for 10 min), incubated with a donkey Alexa Fluor 594 (red) or Alexa Fluor 488 (green) fluorophore-labeled secondary antibody (1:400; Invitrogen) for 1 h 30 min, and washed in PBS (three times for 10 min) before being mounted in an anti-fade mounting solution (Invitrogen). Sections for the DAB reaction were washed in PBS (three times for 10 min), incubated with a biotinylated donkey anti-rabbit secondary antibody (1:400 in PBS containing Triton X-100, 1% donkey serum; Invitrogen) for 1 h 30 min, washed in PBS (three times for 10 min), and incubated with PBS containing the avidin–biotin–peroxidase complex (ABC Elite, 0.2% A and 0.2% B; Vector Laboratories) for 1 h 30 min. After being washed in Tris-HCl buffer (0.05 M, pH 7.5; three times for 10 min), bound peroxidase was revealed by incubation in 0.025% DAB and 0.0006% H_2O_2 in Tris-HCl buffer. Sections were incubated for ~5 min and washed again. Sections were serially mounted, and photomicrographs (bright-field and epifluorescence) were acquired as described above. Confocal photomicrographs were acquired with a confocal microscope (Leica TCS SP5 MP; Leica Microsystems). Alexa Fluor 488 was excited with an argon 543 nm laser, and Alexa Fluor 594 was excited with a helium/neon laser. Images were scanned along the *z*-axis with a frame size of 1024 × 1024 pixels for illustration or 512 × 512 for cell counting (Fox3/GAD).

tVTA cell counting. Sections (40-μm-thick) at 160 μm intervals throughout the VTA/tVTA (−5.6 to −7.6 mm from posterior to bregma) were processed for Fox3 and GAD double-immunofluorescence staining (three rats). A 20× objective was used to acquire two z stacks per section (one per hemisphere) in the VTA/tVTA area. After acquisition, NIH ImageJ was used to manually quantify the proportion of tVTA neurons ($Fox3^+$) that were GABAergic (GAD^+). After confocal acquisition, sections were counterstained with neutral red (Thermo Fisher Scientific) to accurately evaluate distance from bregma. The mean proportion of VTA/tVTA neurons that were GABAergic was plotted as a function of their position posterior to bregma (Fig. 1*A*). This quantification allowed us to define the appropriate area in the tVTA to target in electrophysiological recordings.

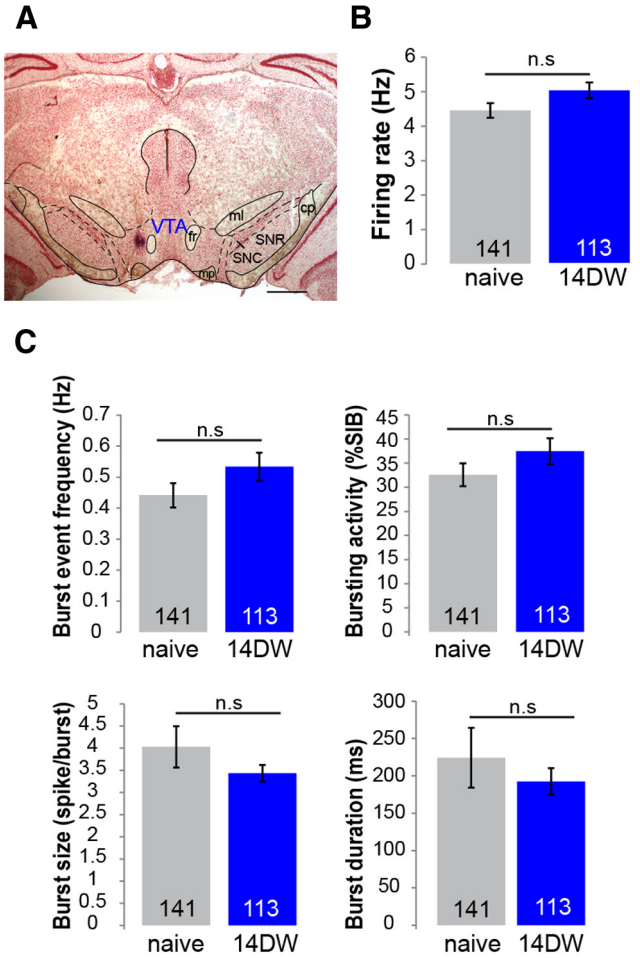

Figure 3. The firing of VTA DA neurons is the same in naive and PW rats. ***A***, Photograph showing a pontamine sky blue deposit that marks a recording site in the VTA. Scale bar, 1 mm. ***B***, Bar graph showing that the mean basal firing rate of VTA DA neurons in naive and 14DW rats is similar. ***C***, Analyses of VTA DA neuron busting activity. Bars graphs show that bursting activity is similar between VTA DA neurons in naive and 14DW rats. For all figures: naive/placebo rats, $n = 141$ cells, 39 rats; 14DW rats, $n = 114$ cells, 25 rats. cp, cerebral peduncle; fr, fasciculus retroflexus; ml, medial lemniscus; mp, mammillary peduncle; %SIB, percentage of spikes in bursts; SNC, substantia nigra pars compacta; SNR, substantia nigra pars reticulata.

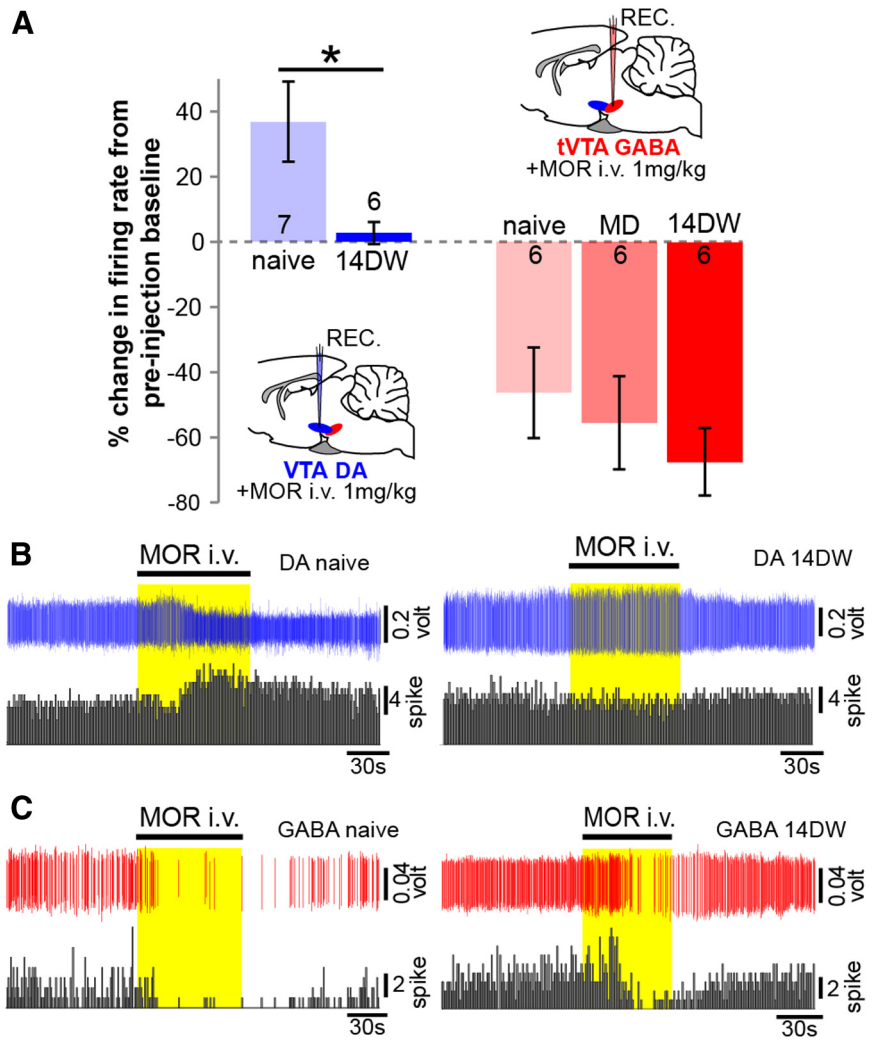

Figure 4. Intravenous morphine modulates tVTA GABA neurons in naive, MD, and acute withdrawal rats but has no effect on VTA DA neurons during withdrawal. ***A***, Bar graph and schematics illustrating the effect of intravenous morphine (MOR; 1 mg/kg) on VTA DA and tVTA GABA neuronal activity during morphine treatment. Morphine activates DA VTA neurons in naive but not in 14DW rats (blue bars). Conversely, morphine inhibits tVTA GABA neurons in naive as well as in MD and 14DW rats, with no differences between these groups. VTA DA recording: naive rats, $n = 7$; 14DW rats, $n = 6$; tVTA GABA recording: naive rats, $n = 6$; MD rats, $n = 6$; 14DW rats, $n = 6$. ***B***, Example traces (in blue) and firing rate histograms (in dark gray) from a naive VTA DA neuron (left) and a 14DW VTA DA neuron (right). The examples show the typical increased firing activity after morphine injection in naive but not in 14DW rat neurons. ***C***, Example traces (in blue) and firing rate histogram (in dark gray) from tVTA GABA neurons recorded in a naive rat (left) or a 14DW tVTA rat (right) showing decreased firing activity after morphine injection in both cases. *$p < 0.05$.

Data analysis. To compare basal firing rates of tVTA GABA neurons and VTA DA neurons, each cell was recorded for at least 120 s. In addition, burst analysis was performed on putative DA VTA neurons. The onset of a burst was defined as the occurrence of two spikes with an interspike interval <80 ms (Grace and Bunney, 1984a). The percentage of spikes in bursts was calculated by dividing the number of spikes occurring in bursts (first spike of the burst not included) by the total number of spikes occurring in the same period of time. Drug-induced changes in burst firing are reported as the percentage of spikes in bursts before the drug minus the percentage after the drug. We also evaluated the amount of bursting activity by calculating the burst-event frequency (number of burst events over time), the burst size (number of spikes within each burst), and the duration of each burst.

To analyze the effect of intravenous morphine injection on putative DA VTA and GABA tVTA neurons, basal activity 60 s before versus after injection were compared. For local drug microinjections, basal neuronal activity in the 30 s epochs before versus after injections was compared.

During photostimulation of the tVTA, cumulative peristimulus time histograms (PSTHs; 5 ms bin width) of VTA/tVTA activity were generated for each recorded neuron. PSTHs were analyzed to determine inhibitory and excitatory epochs as described previously (Georges and Aston-Jones, 2002; Moorman and Aston-Jones, 2010). The mean and SD of counts per bin were determined for a baseline period (500 ms epoch preceding stimulation). Inhibition was defined as an epoch of at least three bins in which the mean count per bin was at least 35% less than that during baseline. The onset of significant excitation was defined as the first bin for which the mean value exceeded mean baseline activity by 2 SDs, and response offset was determined as the time at which activity had returned to be consistently within 2 SDs of baseline. During tVTA stimulation with VTA recording, only inhibition was observed, and latency and duration of inhibitory responses were compared between naive and 14DW rats.

In all cases, results are expressed throughout as mean ± SEM. When two means were compared, the statistical significance of their difference was assessed by two-tailed paired Student's *t* tests. For multiple comparisons, values were subjected to a one-way ANOVA, followed by *post hoc* Newman–Keuls tests. All measurements and analyses were performed in Spike2 (Cambridge Electronic Design), SPSS (IBM), or Excel (Microsoft).

Results

Identification and localization of putative GABA neurons in the tVTA

Our immunohistochemical results confirmed previous findings that the tVTA is rich in GABA (GAD^+) neurons and μ opioid receptors (Jhou et al., 2009b; Kaufling et al., 2009; Fig. 1*F*). We also performed double immunostaining for Fox3 (to identify neurons) and GAD through the VTA and tVTA (Fig. 1*C*) to evaluate the proportion of tVTA neurons that are GABAergic. These experiments revealed that >75% of tVTA neurons are GABAergic (Fig. 1*D*). We additionally used sections stained for GAD and μ receptors in coronal sections throughout the rostrocaudal extent of the VTA and tVTA to confirm neuronal recording sites (Figs. 1*A*,*B*, 2).

Differential basal firing rates for VTA DA versus tVTA GABA neurons during protracted morphine withdrawal

We obtained single-unit recordings from the region of the tVTA in 91 rats under isoflurane anesthesia. We identified putative DA neurons (denoted hereafter as DA neurons; but see Materials and Methods for limitations) based on waveform duration (<1.1 ms to negative trough, >2.5 ms for full waveform) and basal firing rate (<10 spikes/s; Fig. 1*D*), as reported previously (Grace and Bunney, 1984b; Ungless et al., 2004, Luo et al., 2008). This revealed that ~12% of neurons from our tVTA recordings were putatively DA. We identified putative GABAergic neurons (denoted hereafter as GABA neurons) in tVTA by their narrow waveforms (<1.1 ms to

negative trough) and lack of spontaneous burst firing. Based on this, 274 of the 312 (88%) neurons we recorded in tVTA were putatively GABAergic (Fig. 1*E*); this is consistent with the high percentage of GAD$^+$ neurons we identified in this same region (above).

The position of each tVTA neuron recorded was plotted on drawings of coronal sections through the tVTA (Fig. 2*A*). The application of two blue spots (Fig. 2*B*) allowed us to accurately determine the position of recorded cells. This analysis confirmed similar locations of recorded neurons in each experimental group of our study. The comparison of the action potential durations between groups also did not differ ($F_{(3,269)} = 2.02, p > 0.1$) and confirmed that our treatments did not alter the waveforms of tVTA neurons (Fig. 2*C*). We compared the basal firing rates of putative tVTA GABA neurons between groups of rats given acute or chronic morphine treatments or during morphine withdrawal (Fig. 2).

Basal firing rates for tVTA neurons did not differ between naive rats and animals given placebo pellets, which allowed us to pool these control data. However, ANOVA revealed that the average firing rates of tVTA GABA neurons differed among experimental groups ($F_{(3,269)} = 9.5, p = 0.001$; Fig. 2*D*), with significantly lower basal activity of tVTA neurons in MD rats (2.9 ± 0.5 ms) compared with naive/placebo rats (7.8 ± 1.2 ms). NAL-precipitated withdrawal (7.5 ± 1.1 ms) "normalized" the firing of tVTA neurons, which was then not significantly different from naive/placebo animals. Interestingly, this "normalization" was transient: after 14 d of morphine abstinence withdrawal (14DW, PW), the basal firing rate of tVTA GABA neurons (4.1 ± 0.6 ms) was similar to that in MD rats and significantly lower than in naive/placebo subjects. This last result was unexpected, because tVTA GABA neurons regulate VTA DA neural activity in naive animals (Bourdy and Barrot, 2012), and Georges et al. (2006) found increased firing in VTA DA neurons in MD rats but a normalization of this firing in both PW and 14DW rats. Together with our results above, these findings indicate that the control of VTA DA neurons by tVTA GABA neurons is altered in 14DW animals. We recorded VTA DA cells in naive and 14DW rats to verify this altered tVTA–VTA relationship (Fig. 3). In contrast to the above results for tVTA GABA neurons, we confirmed that there was no significant difference between DA neurons in naive versus 14DW rats in terms of mean basal firing rate ($t_{(253)} = 0.075, p > 0.001$; Fig. 3*B*) or bursting parameters (burst event frequency: $t_{(253)} = 0.136, p > 0.1$; bursting activity: $t_{(253)} = 0.225, p > 0.1$; burst size: $t_{(253)} = 0.243, p > 0.1$; burst duration: $t_{(253)} = 0.463, p > 0.1$; Fig. 3*C*).

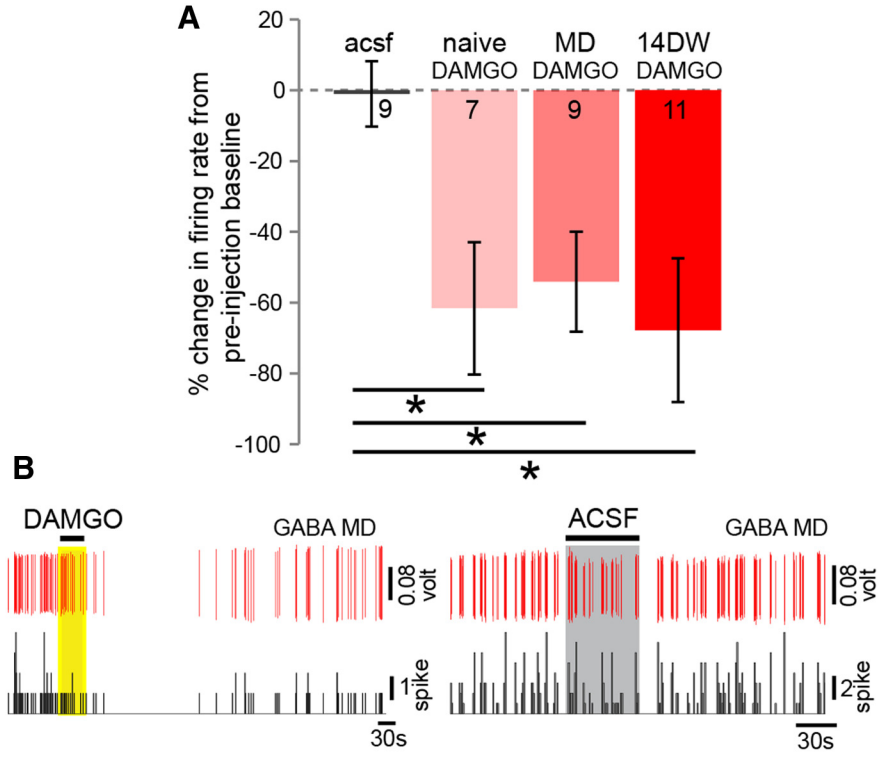

Figure 5. Local μ receptor agonist inhibits tVTA GABA neurons in naive, MD, and PW rats. ***A***, Bar graph reveals that local microinjections of DAMGO inhibit tVTA GABA neurons in naive, MD, and 14DW rats. Note that vehicle injections (ACSF) do not modify neuronal activity. ACSF injections: $n = 9$ cells, 4 rats (3 naive, 1 MD); DAMGO injection: naive rats, $n = 10$ cells, 7 rats; MD rats, $n = 9$ cells, 4 rats; 14DW rats, $n = 11$ cells, 5 rats. ***B***, Examples of raw spike traces (in red) and firing rate histograms (in black) from two tVTA GABA neurons recorded in MD rats showing decreased firing activity after DAMGO injection (left) and the lack of effect after vehicle injection (right). *$p < 0.05$.

Acute opiate administration reveals tolerance in VTA DA neurons but not in tVTA GABA neurons

We next sought to determine whether tVTA GABA and VTA DA neurons express apparent morphine tolerance after chronic morphine treatment and morphine withdrawal. For this, we acutely administered morphine (1 mg/kg, i.v.) during recordings from VTA or tVTA neurons (Fig. 4). As shown previously (Georges et al., 2006), acute morphine increased impulse activity of DA neurons in VTA in naive rats (36.8 ± 12.3%) but not in 14DW rats (2.6 ±3.4%, $t_{(11)} = 2.49, p = 0.03$; Fig. 4*A*,*B*), revealing apparent tolerance in these cells. In contrast, GABAergic neurons in the tVTA were similarly inhibited by acute morphine in naive, MD, and 14DW rats (by −46.3 ± 13.8, −55.4 ± 14.2, and −67.4 ± 10.4%, respectively, $F_{(2,15)} = 0.67, p > 0.1$; Fig. 4*A*,*C*), revealing that these neurons do not exhibit apparent tolerance.

We also tested the sensitivity of tVTA neurons to direct μ receptor stimulation using a double-barrel micropipette to locally apply the specific μ opioid agonist DAMGO (100 μM, 60 nl) on recorded cells (Fig. 5). These microinjections reduced tVTA impulse activity to a similar extent in naive (−62.1 ± 15.1%, 10 neurons), MD (−54.1 ± 14.1%, nine neurons) and 14DW (−77.9 ± 11.2%, 11 neurons) rats. Similar microinjection of vehicle (ACSF) did not significantly modify tVTA GABA neuron activity (−1.1 ± 9.2%, $F_{(3,35)} = 6.8, p = 0.001$; Fig. 5*B*). These experiments confirmed the presence of μ receptors on tVTA GABA neurons and the lack of morphine tolerance in these cells after chronic treatment and withdrawal or abstinence. This lack of tolerance of tVTA GABA neurons compared with the apparent tolerance in VTA DA neurons confirmed decreased regulation of VTA DA neurons by tVTA inputs after protracted morphine withdrawal.

tVTA optogenetic stimulation reduced VTA DA activity similarly in naive and 14DW rats

Several studies showed that tVTA stimulation inhibits VTA DA neurons in naive animals (Jalabert et al., 2011; Matsui and Wil-

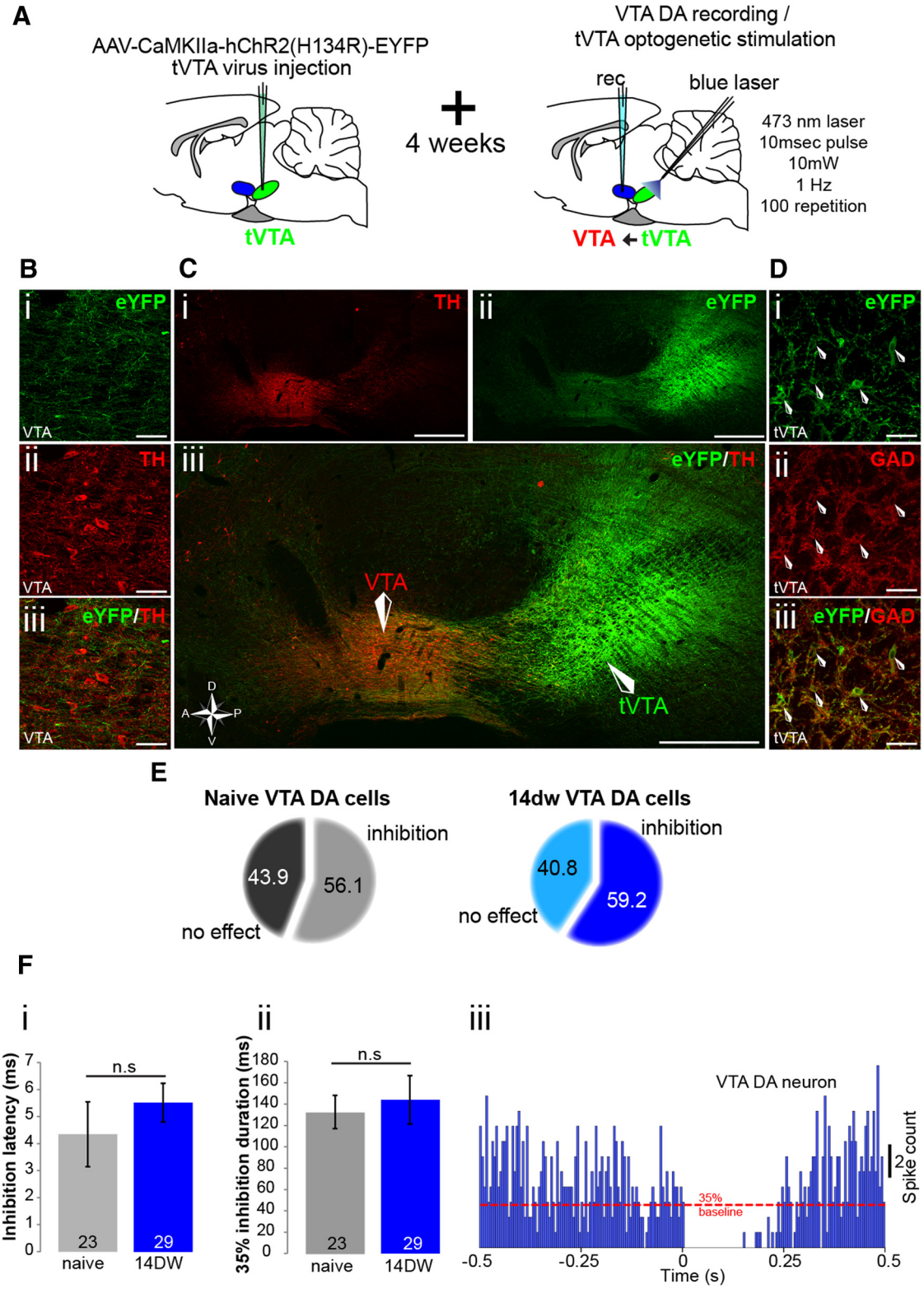

Figure 6. tVTA optogenetic activation inhibits VTA DA-like neurons in naive and PW rats. ***A***, Schematics illustrate the virus injection protocol (left) and the photostimulation recording protocol (right). VTA DA neurons recorded during tVTA optogenetic stimulation. ***B***, Fluorescence photographs of VTA sagittal sections showing immunofluorescent staining for eYFP (tag to mark ChR2 expression; ***i***), TH (***ii***), and merge (TH/eYFP; ***iii***), showing ChR2 $^{+}$ tVTA afferent fibers around VTA DA neurons after a tVTA virus injection. Scale bar, 1 mm. ***C***, Fluorescence photographs of photomontaged sagittal sections showing the tVTA and VTA. Immunofluorescent staining for TH (***i***), eYFP (***ii***), and merge (***iii***). Note that the virus-infected area (green) is restricted to the tVTA region. There is no contamination of VTA DA neurons. Scale bar, 500 μm. ***D***, Fluorescence photomicrographs of tVTA sagittal sections showing immunofluorescent staining for eYFP (***i***), GAD (***ii***), and merge (***iii***), showing tVTA GABA neurons that express ChR2 (white arrows). Scale bar, 1 mm. ***E***, Pie charts represent the fraction of VTA DA recorded neurons responding to tVTA photostimulation in naive and 14DW rats that express ChR2 in tVTA. Note that the proportion of DA VTA responding neurons, ~60%, is similar in the two groups. Naive rats, 23 of 41 inhibited cells; 14DW rats, 29 of 49 inhibited cells. ***F***, Bar graphs illustrating latencies (***i***) and durations (***ii***) for VTA DA neurons in naive and 14DW rats inhibited at least 35% after photostimulation of ChR2-expressing tVTA neurons. There were no significant differences between groups. ***iii***, PSTH illustrating a typical example from a naive rat of a VTA DA neuron inhibited by tVTA photostimulation (at time 0).

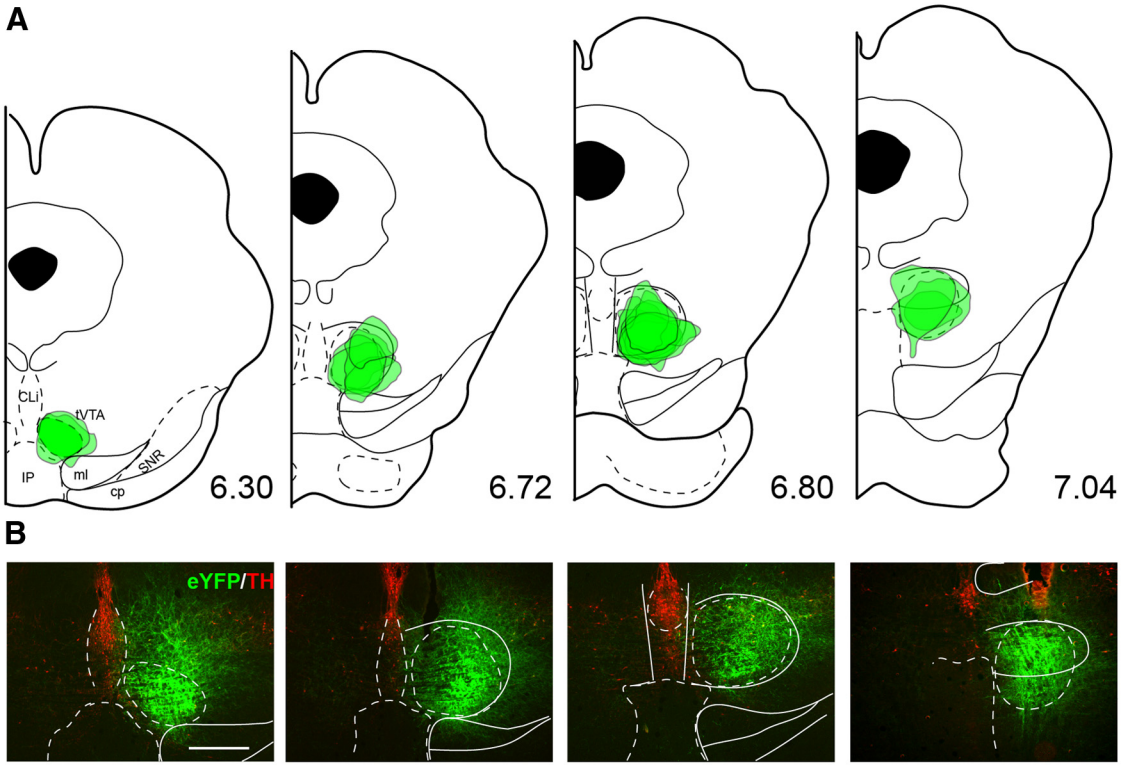

Figure 7. Expression of ChR2 in the tVTA for optogenetic experiments. ***A***, Virus expression sites are plotted on four frontal sections from a rat brain atlas (Paxinos and Watson, 2007). Each viral site ($n = 18$) is presented at the level of its maximal extent. Approximate anteroposterior distance to bregma (in millimeters) is indicated on each drawing. ***B***, Four examples of ChR2 expression in the tVTA. ChR2 expression was revealed using eYFP histochemistry. TH staining was added as a counterstain. CLi, caudal linear nucleus of the raphe; cp, cerebral peduncle; IP, interpeduncular nucleus; ml, medial lemniscus; SNR, substantia nigra pars reticulata.

liams 2011; Lecca et al., 2012). To compare the effect of tVTA stimulation on putative VTA DA neurons in naive and 14DW rats, we expressed the cation channel ChR2 in tVTA neurons by injecting an AAV that encoded ChR2 fused to eYFP reporter (ChR2–eYFP) into the tVTA *in vivo* (Fig. 6). This virus construct was driven by a CaMKII promoter, which we used because recent work obtained strong ChR2 expression in subcortical GABA neurons using a similar promoter (Sohal et al., 2009; Stuber et al., 2011; Tye et al., 2011). To validate viral expression selectively in tVTA GABA neurons, we performed eYFP/TH and eYFP/GAD immunohistochemistry in VTA and tVTA regions of injected animals (Fig. 6*B–D*). Small-volume virus injections (60 nl) allowed us to contain ChR2 expression to tVTA and to avoid substantial VTA DA contamination (Figs. 6*B–D*, 7).

A

	tVTA optogenetic stimulation
Excitation onset latency (ms)	2.67 + 0.80
Excitation duration (ms)	7.5 + 1.70
Response magnitude (spike)	82 + 9.42
Proportion of excited neuron	6/6

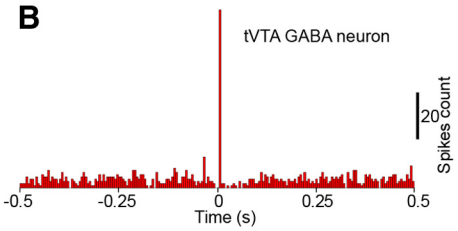

Figure 8. ChR2 stimulation excites tVTA GABA neurons. ***A***, Table showing the effect of tVTA optogenetic stimulation on tVTA GABA neurons. As expected, tVTA putative GABA neurons are stimulated by the tVTA stimulation. $n = 6$ cells, 2 naive rats. ***B***, PSTH illustrating a typical example of tVTA short-latency responses to local tVTA photostimulation (at time 0).

We observed that a large population of tVTA cells expressed ChR2 and were GAD$^+$ and that ChR2$^+$ efferent processes were located in the vicinity of VTA DA neurons (Fig. 6*B*). We photostimulated the tVTA with a blue laser (473 nm laser, 10 ms pulse, 10 mW, 1 Hz, 100 repetitions) during VTA DA recording at least 4 weeks after virus injection using an optical fiber placed 400 μm above the site of virus injection in the tVTA. In an additional group of animals, a recording pipette glued 500 μm below the optic fiber tip allowed us to record tVTA GABA neurons during photostimulation and confirmed that our protocol stimulated tVTA GABA neurons (Fig. 8).

In naive animals, 56.1% of VTA DA neurons were inhibited during tVTA photostimulation (Fig. 6*E*,*F*). There was no difference in the effects of tVTA photostimulation on activity of VTA DA neurons between naive and 14DW rats: a similar proportion of neurons were inhibited (56.1 vs 59.2%), the latencies of inhibition were similar (4.3 ± 1.2 vs 5.5 ± 0.7 ms; $t_{(50)} = 0.386$, $p > 0.1$), as were the durations of inhibition (132.6 ± 15.5 vs 144.1 ± 22.7 ms; $t_{(50)} = 0.585$, $p > 0.1$; Fig. 6*F*). These results showed that protracted morphine withdrawal did not alter the influence of tVTA input to VTA DA neurons, because tVTA stimulation similarly inhibited VTA DA neurons in both naive and 14DW rats.

tVTA inactivation enhanced VTA DA activity in naive but not in 14DW rats

As described above, protracted morphine withdrawal decreased activity in tVTA neurons without affecting VTA DA neuron firing, and the VTA DA inhibition induced by tVTA stimulation was not altered after protracted morphine withdrawal. To better understand these results, we pharmacologically inhibited tVTA neurons by microinjecting the fluorescently labeled $GABA_A$ agonist MusB into the tVTA (0.8 mM/0.5 μl; Jalabert et al., 2011). We

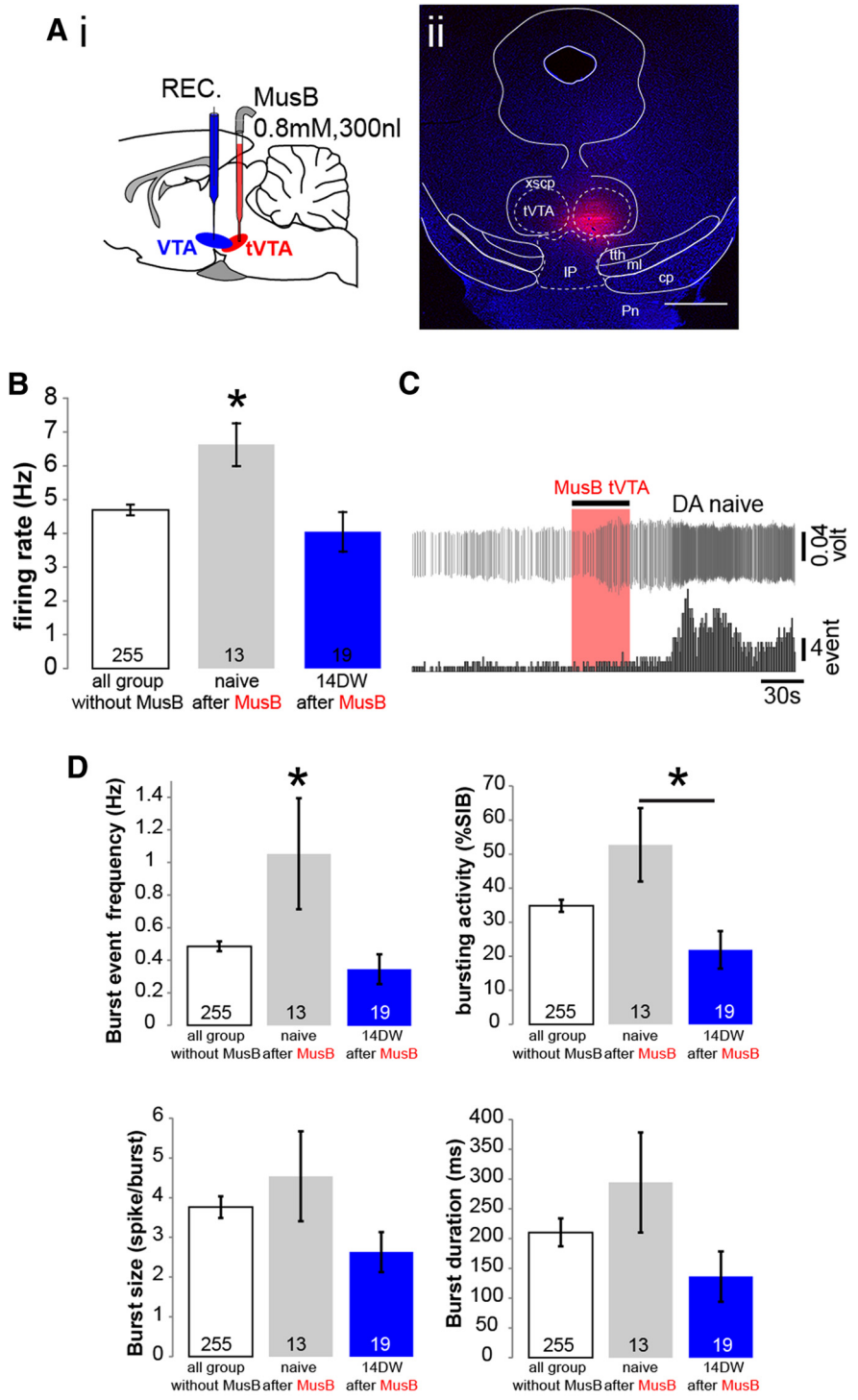

Figure 9. Inactivation of tVTA neurons activates VTA DA-like neurons in naive but not in withdrawal rats. ***Ai***, Schematic illustrates local MusB microinjection (0.8 mM, 500 nl) during VTA DA neural recording. ***Aii***, Photograph of a frontal section through the tVTA showing an example MusB injection. Scale bar, 1 mm. ***B***, Bar graph reveals the increase of activity in VTA DA-like neurons in naive but not in 14DW rats after tVTA MusB injection. ***C***, Example trace (top) and firing rate histogram (bottom) from a naive VTA DA neuron showing the typical increased firing activity after tVTA MusB microinjection. ***D***, Analysis of VTA DA neuron busting activity parameters. Bar graphs show that bursting in VTA DA-like neurons is increased after tVTA MusB injection in naive but not in 14DW rats. For all graphs: without MusB, $n = 255$ cells, 64 rats; after MusB: naive rats, $n = 13$ cells, 7 rats; 14DW rats, $n = 19$ cells/5 rats. $^*p < 0.05$. cp, cerebral peduncle; IP, interpeduncular nucleus; ml, medial lemniscus; Pn, pontine nuclei; tth, trigeminothalamic tract; tVTA, tail of the ventral tegmental area; xscp, decussation of the superior cerebellar peduncle.

then recorded VTA DA neurons during 2 h post-injection in naive or 14DW rats (Fig. 9). The fluorescent tag linked to the MusB allowed us to histologically confirm the localization of the MusB injection sites in tVTA (Fig. 9*A*). Unlike with tVTA stimulation, there were different effects of tVTA inhibition on VTA DA neural activity in naive versus 14DW animals: tVTA inhibition activated VTA DA neurons in naive rats (as expected) but failed to have any effect in 14DW rats (Fig. 9*B*). Mean basal firing rate and bursting activity of VTA DA neurons in naive rats were significantly higher after MusB injection than in naive rats without MusB injection or than in 14DW rats with or without MusB injections (firing rate: $F_{(2,283)} = 4.5$, $p = 0.012$; burst event frequency: $F_{(2,283)} = 8.1$, $p = 0.000$; bursting activity: $F_{(2,283)} = 4.46$, $p = 0.012$; burst size: $F_{(2,283)} = 0.9$, $p = 0.41$, $p > 0.1$; burst duration: $F_{(2,283)} = 0.7$, $p = 0.41$, $p > 0.1$; Fig. 9*B*,*D*). Thus, during protracted withdrawal, stimulation of the tVTA GABA neurons inhibited VTA DA neurons, but inactivation of tVTA had no effect on DA cells.

Morphine withdrawal reduced glutamatergic tone in VTA

The findings above led us to hypothesize that morphine withdrawal might reduce resting excitatory (possibly glutamatergic) tone in the VTA and that this might underlie in part the finding that DA neurons fire at a normal rate during PW despite reduced tonic activity of tVTA neurons (described above). Such a lack of glutamate tone could also underlie the lack of excitation of VTA DA neurons by acute inhibition of tVTA or by acute morphine during withdrawal in our results above. To test this possibility, we locally microinjected a mixture of AMPA and NMDA glutamate antagonists (50 μM CNQX plus 100 μM AP-5; 60 nl) onto recorded VTA DA neurons in naive or 14DW rats. As shown in Figure 10, this antagonist mixture significantly reduced the basal firing rate of VTA DA neurons in naive rats ($-31.2 \pm 5.6\%$) during the 30 s after compared with before microinjection but had no significant effect in 14DW animals ($-9.0 \pm 2.4\%$ during the same time period; $F_{(2,44)} = 18.3$, $p = 0.0001$). Similar vehicle microinjection had no significant effect in naive rats (ACSF, $-0.7 \pm 2.6\%$; Fig. 10*B*,*C*). These results support our hypothesis that morphine withdrawal reduces tonic excitatory glutamate tone on VTA DA neurons. Together with the above finding that withdrawal decreases

tVTA-induced inhibitory tone on VTA DA neurons, this result offers an explanation for why, during protracted withdrawal, (1) VTA DA neurons fire at the same rate as in naive rats and (2) acute morphine does not activate VTA DA neurons despite inhibition of tVTA neurons.

Discussion

VTA DA neurons are indirectly activated by μ opiates via a disinhibitory process, at least in part, resulting from inhibition of a resting GABA tone. The tVTA provides a strong GABA input to DA neurons and participates in generating such an inhibitory tone (Jalabert et al., 2011; Matsui and Williams, 2011; Lecca et al., 2012). Morphine directly inhibits tVTA GABA neurons, and opiates administered into the tVTA produce an indirect activation of VTA DA neurons (Jalabert et al., 2011; Matsui and Williams, 2011; Lecca et al., 2012). However, this picture changes substantially after opiate withdrawal. We confirmed the results of Georges et al. (2006) that VTA DA neurons express morphine tolerance as they become unresponsive to morphine after withdrawal. Nevertheless, we did not observe such tolerance in tVTA GABA neurons. These different adaptations to morphine led us to hypothesize a "functional disconnection" between tVTA GABA and VTA DA neurons during long-term withdrawal. Indeed, we observed that tVTA photostimulation inhibited VTA DA neurons similarly in naive and 14DW subjects but that tVTA inhibition failed to activate DA neurons in 14DW rats. This indicates that inhibitory signaling between tVTA and VTA remains functional but significantly altered during withdrawal. These results led us to hypothesize that the lack of activation of VTA DA neurons after opiate-induced inhibition of tVTA neurons in withdrawn animals involves an additional factor. Indeed, we showed that the resting glutamatergic tone on VTA DA neurons is greatly reduced in 14DW rats. Based on these findings, we propose that VTA DA neurons become unresponsive to acute opiates during withdrawal because of two concomitant factors: (1) decreased tonic tVTA neuronal activity, which produces less disinhibition of DA neurons after opiate-induced inhibition of tVTA GABA neurons; and (2) decreased tonic glutamatergic input to VTA DA neurons. This offsets the loss of tonic GABAergic input from tVTA so that baseline DA neuronal firing rate remains normal and also disallows activation after acutely decreased tVTA GABA input after additional opiate administration.

It is also possible that GABA inputs to VTA DA neurons other than from the tVTA (e.g., nucleus accumbens or VTA interneurons) could also participate in altered responses during withdrawal. For example, Bonci and Williams (1997) described protracted adaptations of GABAergic function in VTA after morphine withdrawal.

tVTA role in VTA DA morphine tolerance

Although attention has focused on the acute effect of opiates on tVTA GABA neurons, our study is the first to investigate *in vivo* the effect of chronic morphine, precipitated morphine withdrawal, and protracted morphine withdrawal on tVTA GABA neurons. Previous dose–response experiments provided evidence that the intravenous dose of 1 mg/kg morphine used here is submaximal for activation of VTA DA *in vivo*. (Melis et al., 2000a, 2000b). Those data support our conclusion that, in contrast to VTA DA neurons, tVTA GABA cells do not express apparent long-term morphine tolerance. Moreover, we found that the lack of activation of DA neurons during withdrawal is not attributable to a disconnection between the VTA and tVTA but rather to altered tVTA GABA and tonic glutamate inputs to the VTA.

In a recent study, Matsui et al. (2014) observed tolerance of VTA DA neurons to morphine in slice recordings after chronic morphine. They proposed that this was attributable to partial morphine tolerance at tVTA terminals on DA neurons. They also observed a smaller increase in the amplitude of GABA IPSCs from the tVTA on VTA DA neurons in "precipitated withdrawal" in slices from chronic morphine rats compared with control animals. Although our experiments support another conclusion, major differences are present between both studies. We used *in vivo* procedures, whereas Matsui et al. (2014) used *in vitro* preparations. In this latter case, afferents to VTA are sectioned and some network influences are lost. Moreover, withdrawal was acutely precipitated in *ex vivo* slices during patch-clamp experiments by direct infusion of naloxone, whereas we removed the *in vivo* source of morphine and waited 2 weeks for protracted withdrawal. Matsui et al. (2014) examined the direct consequences of chronic morphine exposure on receptor function, whereas our study examined long-term *in vivo* adaptations accompanying protracted withdrawal. Together, these data would suggest that, during the history of opiate withdrawal, tolerance at tVTA–VTA synapses may be initially present whereas deficits in glutamater-

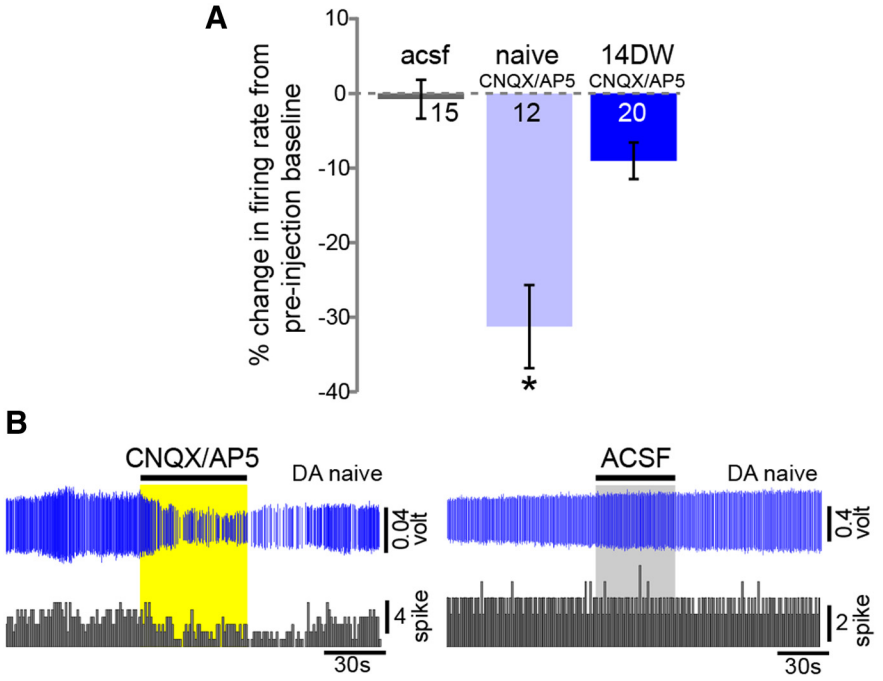

Figure 10. Local glutamate antagonist reveals a reduction of glutamatergic tone in the VTA of withdrawal rats. ***A***, Bar graph illustrates that activity of VTA DA-like neurons is reduced by local CNQX/AP-5 microinjection in naive rats more than in 14DW rats. Note that vehicle (acsf) injections did not modify neuronal activity. ACSF, 19 cells, 4 naive rats; CNQX/AP-5 naive rats, $n = 12$ cells, 3 rats; 14DW rats, $n = 21$ cells, 3 rats. ***B***, Examples of traces (top) and firing rate histograms (bottom) from two VTA DA-like neurons recorded in naive rats showing the typical decrease in activity after CNQX/AP-5 injection (left) and the lack of effect after vehicle injection (right). $*p < 0.05$.

gic inputs and in tVTA firing might underlie the altered VTA DA responsiveness during longer-term protracted withdrawal states.

Glutamate regulation of VTA DA neurons

Glutamatergic transmission is a major component in the regulation of DA neuron activity. VTA NMDA receptors mediate a switch in DA neurons from pacemaker-like to bursting activity (for review, see Lobb et al., 2011), and glutamate in the VTA plays an important role in the actions of many drugs of abuse (Harris and Aston-Jones, 2003a; Bellone and Lüscher, 2006; Mameli et al., 2011; Morikawa and Paladini, 2011; Henny et al., 2012; Kempadoo et al., 2013). Here, we found a reduced glutamatergic tone onto presumed DA neurons during protracted morphine withdrawal. This result is consistent with previous findings that a glutamatergic receptor antagonist applied onto VTA DA neurons in naive rats blocked activation of these cells by acute morphine, showing that such activation requires an underlying glutamate tone (Jalabert et al., 2011). Our findings together with these results lead us to conclude that two major long-term changes during protracted morphine withdrawal prevent DA neurons from being activated by disinhibition from tVTA GABA inputs after acute opiates. (1) tVTA neurons fire spontaneously more slowly, thereby exerting a lower tonic inhibition on VTA DA neurons. This means that opiate-induced inhibition of these cells has less ability to disinhibit DA neurons. However, this decreased tVTA input does not result in higher baseline DA neural activity because of the second, simultaneous change. (2) Tonic glutamate tone on VTA DA neurons is also substantially reduced during protracted withdrawal. This also decreases tonic excitatory drive on DA neurons, so that a loss of inhibitory input produces less activation. Thus, tonic glutamate input to VTA DA neurons plays a significant role in naive rats in DA disinhibition–excitation following the inhibition of tVTA GABA inputs during opiate administration, and loss of this tonic excitatory influence is also a significant factor in the unresponsiveness of DA neurons to acute opiates during withdrawal.

The mechanism responsible for the tonically reduced activity of tVTA neurons during withdrawal is unknown but might also involve reduced glutamate inputs, in parallel with the reduced glutamate tone in VTA DA neurons. The mechanisms responsible for reduced glutamate tone during withdrawal are also unknown but two possibilities seem likely: (1) a postsynaptic effect mediated by a modification of glutamatergic receptors on DA neurons (Saal et al., 2003; Bellone and Lüscher, 2006) or (2) a reduced glutamate tone from afferents to VTA during withdrawal. VTA DA neurons receive glutamatergic afferents from local VTA neurons (Yamaguchi et al., 2007) and also from the prefrontal cortex (Sesack and Pickel, 1992; Murase et al., 1993; Karreman and Moghaddam, 1996; Harden et al., 1998), the bed nucleus of the stria terminalis (Georges and Aston-Jones, 2001; Georges and Aston-Jones, 2002; Jennings et al., 2013), and the pedunculopontine nucleus (Charara et al., 1996; Floresco et al., 2003). A reduction of activity in these inputs could underlie the decreased VTA glutamatergic tone we identified during withdrawal.

Conclusions and perspectives for opiate addiction

These data indicate that, during protracted withdrawal, tVTA may no longer drive VTA DA neurons by disinhibition after acute opiate administration and that the rewarding effects of opiates during withdrawal are mediated by other brain structures. Recent studies indicate that NAc is a good candidate (Cui et al., 2014; Matsui et al., 2014). Interestingly, Cui et al. (2014) showed that re-expression of μ opioid receptors in the NAc in μ receptor knock-out mice is sufficient to partially restore opiate place preference, self-administration, and sensitization. The neuroanatomical substrate for opiate reward is thus not restricted to their disinhibitory action on DA cells.

Drug addiction is a chronic brain disorder, with deleterious consequences for individuals and their social environment, including the difficulty to remain abstinent after long-term withdrawal. Relapse can be precipitated by stress, exposure to drug-associated contexts, or re-exposure to the drug itself (Badiani et al., 2011). Another participating factor is altered emotional homeostasis resulting from drug abstinence (Koob and Volkow, 2010; Lutz and Kieffer, 2013). In rodent, opiate abstinence is characterized by anxiety and depressive symptoms, including lowered mood and anhedonia (Harris and Aston-Jones, 1993; Grella et al., 2009) and social withdrawal (Lutz et al., 2014), but also decreased motivation for natural reinforcers (Zhang et al., 2007) and increased vulnerability to stress (Blatchford et al., 2007). Recently, the tVTA has been shown to participate in avoidance behaviors and in the detection of reward prediction errors (Jhou et al., 2009a; Hong et al., 2011; Stamatakis and Stuber, 2012). Our data suggest that, after long-term opiate withdrawal, the tVTA remains able to inhibit VTA DA neurons but can no longer activate them. These results may suggest that the tVTA could maintain its capacity to transmit negative (aversive) information through DA neuron inhibition but no longer produce positive (rewarding) effects through disinhibition, which may contribute to anhedonic states accompanying protracted opiate withdrawal.

References

Akaoka H, Aston-Jones G (1991) Opiate withdrawal-induced hyperactivity of locus coeruleus neurons is substantially mediated by augmented excitatory amino acid input. J Neurosci 11:3830–3839. Medline

Aston-Jones G, Smith RJ, Sartor GC, Moorman DE, Massi L, Tahsili-Fahadan P, Richardson KA (2010) Lateral hypothalamic orexin/hypocretin neurons: a role in reward-seeking and addiction. Brain Res 1314:74–90. CrossRef Medline

Badiani A, Belin D, Epstein D, Calu D, Shaham Y (2011) Opiate versus psychostimulant addiction: the differences do matter. Nat Rev Neurosci 12:685–700. CrossRef Medline

Bals-Kubik R, Ableitner A, Herz A, Shippenberg TS (1993) Neuroanatomical sites mediating the motivational effects of opioids as mapped by the conditioned place preference paradigm in rats. J Pharmacol Exp Ther 264:489–495. Medline

Barrot M, Sesack SR, Georges F, Pistis M, Hong S, Jhou TC (2012) Braking dopamine systems: a new GABA master structure for mesolimbic and nigrostriatal functions. J Neurosci 32:14094–14101. CrossRef Medline

Bellone C, Lüscher C (2006) Cocaine triggered AMPA receptor redistribution is reversed in vivo by mGluR-dependent long-term depression. Nat Neurosci 9:636–641. CrossRef Medline

Blatchford KE, Diamond K, Westbrook RF, McNally GP (2005) Increased vulnerability to stress following opiate exposures: behavioral and autonomic correlates. Behav Neurosci 119:1034–1041. CrossRef Medline

Bonci A, Williams JT (1997) Increased probability of GABA release during withdrawal from morphine. J Neurosci 17:796–803. Medline

Bourdy R, Barrot M (2012) A new control center for dopaminergic systems: pulling the VTA by the tail. Trends Neurosci 35:681–690. CrossRef Medline

Charara A, Smith Y, Parent A (1996) Glutamatergic inputs from the pedunculopontine nucleus to midbrain dopaminergic neurons in primates: Phaseolus vulgaris-leucoagglutinin anterograde labeling combined with postembedding glutamate and GABA immunohistochemistry. J Comp Neurol 364:254–266. CrossRef Medline

Cui Y, Ostlund SB, James AS, Park CS, Ge W, Roberts KW, Mittal N, Murphy NP, Cepeda C, Kieffer BL, Levine MS, Jentsch JD, Walwyn WM, Sun YE, Evans CJ, Maidment NT, Yang XW (2014) Targeted expression of

μ-opioid receptors in a subset of striatal direct-pathway neurons restores opiate reward. Nat Neurosci 17:254–261. CrossRef Medline

Devine DP, Wise RA (1994) Self-administration of morphine, DAMGO, and DPDPE into the ventral tegmental area of rats. J Neurosci 14:1978–1984. Medline

Di Giovanni G, Di Matteo V, Pierucci M, Esposito E (2008) Serotonin-dopamine interaction: electrophysiological evidence. Prog Brain Res 172:45–71. CrossRef Medline

Fields HL, Hjelmstad GO, Margolis EB, Nicola SM (2007) Ventral tegmental area neurons in learned appetitive behavior and positive reinforcement. Annu Rev Neurosci 30:289–316. CrossRef Medline

Floresco SB, West AR, Ash B, Moore H, Grace AA (2003) Afferent modulation of dopamine neuron firing differentially regulates tonic and phasic dopamine transmission. Nat Neurosci 6:968–973. CrossRef Medline

Frenois F, Cador M, Caille S, Stinus L, Le Moine C (2002) Neural correlates of the motivational and somatic components of naloxone-precipitated morphine withdrawal. Eur J Pharmacol 16:1377–1389. CrossRef Medline

Georges F, Aston-Jones G (2001) Potent regulation of midbrain dopamine neurons by the bed nucleus of the stria terminalis. J Neurosci 21:RC160(1–6). Medline

Georges F, Aston-Jones G (2002) Activation of ventral tegmental area cells by the bed nucleus of the stria terminalis: a novel excitatory amino acid input to midbrain dopamine neurons. J Neurosci 22:5173–5187. Medline

Georges F, Le Moine C, Aston-Jones G (2006) No effect of morphine on ventral tegmental dopamine neurons during withdrawal. J Neurosci 26:5720–5726. CrossRef Medline

Gold LH, Stinus L, Inturrisi CE, Koob GF (1994) Prolonged tolerance, dependence and abstinence following subcutaneous morphine pellet implantation in the rat. Eur J Pharmacol 253:45–51. CrossRef Medline

Grace AA, Bunney BS (1984a) The control of firing pattern in nigral dopamine neurons: burst firing. J Neurosci 4:2877–2890. Medline

Grace AA, Bunney BS (1984b) The control of firing pattern in nigral dopamine neurons: single spike firing. J Neurosci 4:2866–2876. Medline

Grace AA, Floresco SB, Goto Y, Lodge DJ (2007) Regulation of firing of dopaminergic neurons and control of goal-directed behaviors. Trends Neurosci 30:220–227. CrossRef Medline

Grella CE, Karno MP, Warda US, Niv N, Moore AA (2009) Gender and comorbidity among individuals with opioid use disorders in the NESARC study. Addict Behav 34:498–504. CrossRef Medline

Gysling K, Wang RY (1983) Morphine-induced activation of A10 dopamine neurons in the rat. Brain Res 277:119–127. CrossRef Medline

Harden DG, King D, Finlay JM, Grace AA (1998) Depletion of dopamine in the prefrontal cortex decreases the basal electrophysiological activity of mesolimbic dopamine neurons. Brain Res 794:96–102. CrossRef Medline

Harris GC, Aston-Jones G (1993) Beta-adrenergic antagonists attenuate withdrawal anxiety in cocaine- and morphine-dependent rats. Psychopharmacology 113:131–136. CrossRef Medline

Harris GC, Aston-Jones G (2003a) Critical role for ventral tegmental glutamate in preference for a cocaine-conditioned environment. Neuropharmacology 28:73–76. CrossRef Medline

Harris GC, Aston-Jones GA (2003b) Altered motivation and learning following opiate withdrawal: evidence for prolonged dysregulation of reward processing. Neuropharmacology 28:865–871. CrossRef Medline

Henny P, Brown MT, Northrop A, Faunes M, Ungless MA, Magill PJ, Bolam JP (2012) Structural correlates of heterogeneous in vivo activity of midbrain dopaminergic neurons. Nat Neurosci 15:613–619. CrossRef Medline

Hjelmstad GO, Xia Y, Margolis EB, Fields HL (2013) Opioid modulation of ventral pallidal afferents to ventral tegmental area neurons. J Neurosci 33:6454–6459. CrossRef Medline

Hong S, Jhou TC, Smith M, Saleem KS, Hikosaka O (2011) Negative reward signals from the lateral habenula to dopamine neurons are mediated by rostromedial tegmental nucleus in primates. J Neurosci 31:11457–11471. CrossRef Medline

Jalabert M, Bourdy R, Courtin J, Veinante P, Manzoni OJ, Barrot M, Georges F (2011) Neuronal circuits underlying acute morphine action on dopamine neurons. Proc Natl Acad Sci U S A 108:16446–16450. CrossRef Medline

Jennings JH, Sparta DR, Stamatakis AM, Ung RL, Pleil KE, Kash TL, Stuber GD (2013) Distinct extended amygdala circuits for divergent motivational states. Nature 496:224–228. CrossRef Medline

Jhou TC, Fields HL, Baxter MG, Saper CB, Holland PC (2009a) The rostromedial tegmental nucleus (RMTg), a GABAergic afferent to midbrain dopamine neurons, encodes aversive stimuli and inhibits motor responses. Neuron 61:786–800. CrossRef Medline

Jhou TC, Geisler S, Marinelli M, Degarmo BA, Zahm DS (2009b) The mesopontine rostromedial tegmental nucleus: a structure targeted by the lateral habenula that projects to the ventral tegmental area of Tsai and substantia nigra compacta. J Comp Neurol 513:566–596. CrossRef Medline

Jhou TC, Xu SP, Lee MR, Gallen CL, Ikemoto S (2012) Mapping of reinforcing and analgesic effects of the mu opioid agonist endomorphin-1 in the ventral midbrain of the rat. Psychopharmacology 224:303–312. CrossRef Medline

Johnson SW, North RA (1992a) Opioids excite dopamine neurons by hyperpolarization of local interneurons. J Neurosci 12:483–488. Medline

Johnson SW, North RA (1992b) Two types of neurone in the rat ventral tegmental area and their synaptic inputs. J Physiol 450:455–468. CrossRef Medline

Karreman M, Moghaddam B (1996) The prefrontal cortex regulates the basal release of dopamine in the limbic striatum: an effect mediated by ventral tegmental area. J Neurochem 66:589–598. CrossRef Medline

Kaufling J, Veinante P, Pawlowski SA, Freund-Mercier MJ, Barrot M (2009) Afferents to the GABAergic tail of the ventral tegmental area in the rat. J Comp Neurol 513:597–621. CrossRef Medline

Kempadoo KA, Tourino C, Cho SL, Magnani F, Leinninger GM, Stuber GD, Zhang F, Myers MG, Deisseroth K, de Lecea L, Bonci A (2013) Hypothalamic neurotensin projections promote reward by enhancing glutamate transmission in the VTA. J Neurosci 33:7618–7626. CrossRef Medline

Koob GF, Volkow ND (2010) Neurocircuitry of addiction. Neuropsychopharmacology 35:217–238. CrossRef Medline

Lavezzi HN, Zahm DS (2011) The mesopontine rostromedial tegmental nucleus: an integrative modulator of the reward system. Basal Ganglia 1:191–200. CrossRef Medline

Lecca S, Melis M, Luchicchi A, Ennas MG, Castelli MP, Muntoni AL, Pistis M (2011) Effects of drugs of abuse on putative rostromedial tegmental neurons, inhibitory afferents to midbrain dopamine cells. Neuropsychopharmacology 36:589–602. CrossRef Medline

Lecca S, Melis M, Luchicchi A, Muntoni AL, Pistis M (2012) Inhibitory inputs from rostromedial tegmental neurons regulate spontaneous activity of midbrain dopamine cells and their responses to drugs of abuse. Neuropsychopharmacology 3:1164–1176. Medline

Lobb CJ, Troyer TW, Wilson CJ, Paladini CA (2011) Disinhibition bursting of dopaminergic neurons. Front Syst Neurosci 5:25. CrossRef Medline

Luo AH, Georges FE, Aston-Jones GS (2008) Novel neurons in ventral tegmental area fire selectively during the active phase of the diurnal cycle. Eur J Neurosci 27:408–422. CrossRef Medline

Lüscher C, Malenka RC (2011) Drug-evoked synaptic plasticity in addiction: from molecular changes to circuit remodeling. Neuron 69:650–663. CrossRef Medline

Lutz PE, Kieffer BL (2013) Opioid receptors: distinct roles in mood disorders. Trends Neurosci 36:195–206. CrossRef Medline

Lutz PE, Ayranci G, Chu-Sin-Chung P, Matifas A, Koebel P, Filliol D, Befort K, Ouagazzal AM, Kieffer BL (2014) Distinct mu, delta, and kappa opioid receptor mechanisms underlie low sociability and depressive-like behaviors during heroin abstinence. Neuropsychopharmcology 39L2694–2705 CrossRef

Mameli M, Bellone C, Brown MT, Lüscher C (2011) Cocaine inverts rules for synaptic plasticity of glutamate transmission in the ventral tegmental area. Nat Neurosci 14:414–416. CrossRef Medline

Margolis EB, Toy B, Himmels P, Morales M, Fields HL (2012) Identification of rat ventral tegmental area GABAergic neurons. PLoS One 7:e42365. CrossRef Medline

Matsui A, Williams JT (2011) Opioid-sensitive GABA inputs from rostromedial tegmental nucleus synapse onto midbrain dopamine neurons. J Neurosci 31:17729–17735. CrossRef Medline

Matsui A, Jarvie BC, Robinson BG, Hentges ST, Williams JT (2014) Separate GABA afferents to dopamine neurons mediate acute action of opioids, development of tolerance, and expression of withdrawal. Neuron 82:1346–1356. CrossRef Medline

Melis M, Diana M, Gessa GL (2000a) Cyclo-oxygenase-inhibitors increase morphine effects on mesolimbic dopamine neurons. Eur J Pharmacol 387:R1–R3. CrossRef Medline

Melis M, Gessa GL, Diana M (2000b) Different mechanisms for dopaminergic excitation induced by opiates and cannabinoids in the rat midbrain. Prog Neuropsychopharmacol Biol Psychiatry 24:993–1006. CrossRef Medline

Moorman DE, Aston-Jones G (2010) Orexin/hypocretin modulates response of ventral tegmental dopamine neurons to prefrontal activation: diurnal influences. J Neurosci 30:15585–15599. CrossRef Medline

Morikawa H, Paladini CA (2011) Dynamic regulation of midbrain dopamine neuron activity: intrinsic, synaptic, and plasticity mechanisms. Neuroscience 198:95–111. CrossRef Medline

Murase S, Grenhoff J, Chouvet G, Gonon FG, Svensson TH (1993) Prefrontal cortex regulates burst firing and transmitter release in rat mesolimbic dopamine neurons studied in vivo. Neurosci Lett 157:53–56. CrossRef Medline

Paxinos G, Watson C (2007) The rat brain in stereotaxic coordinates, 6th ed. San Diego: Academic Press.

Phillips AG, LePiane FG (1980) Reinforcing effects of morphine microinjection into the ventral tegmental area. Pharmacol Biochem Behav 12: 965–968. CrossRef Medline

Richardson KA, Aston-Jones G (2012) Lateral hypothalamic orexin/hypocretin neurons that project to ventral tegmental area are differentially activated with morphine preference. J Neurosci 32:3809–3817. CrossRef Medline

Saal D, Dong Y, Bonci A, Malenka RC (2003) Drugs of abuse and stress trigger a common synaptic adaptation in dopamine neurons. Neuron 37:577–582. CrossRef Medline

Sesack SR, Pickel VM (1992) Prefrontal cortical efferents in the rat synapse on unlabeled neuronal targets of catecholamine terminals in the nucleus accumbens septi and on dopamine neurons in the ventral tegmental area. J Comp Neurol 320:145–160. CrossRef Medline

Sohal VS, Zhang F, Yizhar O, Deisseroth K (2009) Parvalbumin neurons and gamma rhythms enhance cortical circuit performance. Nature 459: 698–702. CrossRef Medline

Stamatakis AM, Stuber GD (2012) Activation of lateral habenula inputs to the ventral midbrain promotes behavioral avoidance. Nat Neurosci 15: 1105–1107. CrossRef Medline

Stuber GD, Sparta DR, Stamatakis AM, van Leeuwen WA, Hardjoprajitno JE, Cho S, Tye KM, Kempadoo KA, Zhang F, Deisseroth K, Bonci A (2011) Excitatory transmission from the amygdala to nucleus accumbens facilitates reward seeking. Nature 475:377–380. CrossRef Medline

Tye KM, Prakash R, Kim SY, Fenno LE, Grosenick L, Zarabi H, Thompson KR, Gradinaru V, Ramakrishnan C, Deisseroth K (2011) Amygdala circuitry mediating reversible and bidirectional control of anxiety. Nature 471:358–362. CrossRef Medline

Ungless MA, Grace AA (2012) Are you or aren't you? Challenges associated with physiologically identifying dopamine neurons. Trends Neurosci 35: 422–430. CrossRef Medline

Ungless MA, Magill PJ, Bolam JP (2004) Uniform inhibition of dopamine neurons in the ventral tegmental area by aversive stimuli. Science 303: 2040–2042. CrossRef Medline

Volkow ND, Wang GJ, Fowler JS, Tomasi D, Telang F (2011) Addiction: beyond dopamine reward circuitry. Proc Natl Acad Sci U S A 108:15037–15042. CrossRef Medline

Wise RA (1989) Opiate reward: sites and substrates. Neurosci Biobehav Rev 13:129–133. CrossRef Medline

Wise RA (2004) Dopamine, learning and motivation. Nat Rev Neurosci 5:483–494. CrossRef Medline

Yamaguchi T, Sheen W, Morales M (2007) Glutamatergic neurons are present in the rat ventral tegmental area. Eur J Neurosci 25:106–118. CrossRef Medline

Yoburn BC, Chen J, Huang T, Inturrisi CE (1985) Pharmacokinetics and pharmacodynamics of subcutaneous morphine pellets in the rat. J Pharmacol Exp Ther 235:282–286. Medline

Zangen A, Ikemoto S, Zadina JE, Wise RA (2002) Rewarding and psychomotor stimulant effects of endomorphin-1: anteroposterior differences within the ventral tegmental area and lack of effect in nucleus accumbens. J Neurosci 22:7225–7233. Medline

Zhang D, Zhou X, Wang X, Xiang X, Chen H, Hao W (2007) Morphine withdrawal decreases responding reinforced by sucrose self-administration in progressive ratio. Addict Biol 12:152–157. CrossRef Medline